Comparative Analysis of Shockwave Behavior in Bell Nozzles Under Pressures Ration Using CFD Simulations and Taguchi Optimization

TALARI RAJ KUMAR[1], SATISH GEERI[2]
[1] *Student, M. Tech, Department of Mechanical Engineering Pragati Engineering College (Autonomous)*
[2]*Associate Professor, Department of Mechanical Engineering Pragati Engineering College (Autonomous)*

Abstract— The study of shockwave formation in nozzle designs is crucial for optimizing the performance and efficiency of propulsion systems. This research focuses on the comparative analysis of shockwave behavior in single bell nozzles under varying inlet pressures and Ambient pressure. By conducting a detailed computational study, the research aims to observe variations in shockwave formation and their impact on nozzle performance. The methodology involves using advanced computational fluid dynamics (CFD) simulations to analyses shockwave patterns and pressure distributions. The study highlights key performance metrics such as thrust, specific impulse, and flow separation behavior, providing a comprehensive understanding of how nozzle design responds to varying inlet and Ambient pressures. By understanding the nuances of shockwave formation and its effects, engineers can design nozzles that perform optimally across a range of operating conditions, enhancing the reliability and effectiveness of rocket and jet propulsion systems. Taguchi optimization is used to create a Design of Experiments (DOE) for conducting the simulations, and the results are validated using Analysis of Variance (ANOVA) and regression analysis. This approach ensures that the findings are robust and provides a regression equation for predicting nozzle performance under different conditions.

Index Terms- Computational Fluid Dynamics, numerical analysis, optimization, shockwave patterns, Bell Nozzle.

I. INTRODUCTION

Hemp The design and optimization of nozzle configurations play a pivotal role in the performance of propulsion systems used in aerospace applications. Nozzles are integral components that control the expansion and acceleration of exhaust gases, significantly affecting thrust and efficiency. Among various nozzle designs, the single bell nozzle is traditionally used for its simplicity and effectiveness at specific operating conditions However, the bell nozzle has garnered attention for its potential to perform efficiently across a broader range of altitudes, making it a promising candidate for next-generation rocket and jet engines. This research focuses on the comparative analysis of shockwave behaviour in bell nozzles under varying inlet pressures and the ambient pressure. By conducting a detailed computational study, the research aims to observe variations in shockwave formation and their impact on nozzle performance. The methodology involves using advanced computational fluid dynamics (CFD) simulations to analyses shockwave patterns and pressure distributions. The study highlights key performance metrics such as thrust, specific impulse, and flow separation behaviour, providing a comprehensive understanding of how nozzle design responds to varying inlet and outlet pressures. By understanding the nuances of shockwave formation and its effects, engineers can design nozzles that perform optimally across a range of operating conditions, enhancing the reliability and effectiveness of rocket and jet propulsion systems. Taguchi optimization is used to create a Design of Experiments (DOE) for conducting the simulations, and the results are validated using Analysis of Variance (ANOVA) and regression analysis. This approach ensures that the findings are robust and provides a regression equation for predicting nozzle performance under different conditions.

The single bell nozzle, also known as the conical or parabolic nozzle, has been extensively studied and optimized for specific mission profiles. Anderson [1] discusses the fundamental principles of nozzle flow dynamics, emphasizing the relationship between nozzle shape and performance parameters such as thrust and specific impulse. The single bell nozzle

design is well-suited for applications where operating conditions remain relatively constant. In contrast, the dual bell nozzle design aims to extend the performance envelope by incorporating two expansion bell sections. This design allows for an adaptive nozzle area ratio, making it more versatile across different altitudes. Hagemann et al. [2] conducted pioneering work on dual bell nozzles, demonstrating their potential for enhanced performance in variable atmospheric conditions. Their research highlighted the benefits of dual bell nozzles in reducing flow separation and improving overall efficiency. Shockwave behavior in nozzles has been a subject of extensive research due to its impact on propulsion efficiency. Hornung [3] provides a comprehensive analysis of shockwave interactions in high-speed flows, explaining the mechanisms leading to flow separation and efficiency loss. Recent advancements in computational fluid dynamics (CFD) have enabled more detailed studies of shockwave phenomena in nozzles. For instance, Greschik and Gruber [4] utilized CFD simulations to investigate shockwave patterns in various nozzle geometries, offering valuable insights into their aerodynamic performance. Moreover, the influence of inlet pressure on shockwave formation is a critical aspect of nozzle design. Studies by Dutton and Carroll [5] examined the effects of varying inlet pressures on shockwave structures in convergent-divergent nozzles, providing a foundation for understanding how different pressures impact nozzle performance.

Many researchers endeavour to stimulate supersonic flow through rocket nozzles with combustion chambers, aiming to comprehend flow dynamics and the variation of flow properties within the ignition chamber. Raja et al. [6] conducted a study on the peculiarities of a Convergent-Divergent (C-D) nozzle using Computational Fluid Dynamics (CFD), concluding it as optimal for low area ratio rocket designs. Kumaar and Kesavan [7] analysed different shock wave behaviours in convergent and divergent nozzles, emphasizing that shockwave propagation depends on Nozzle Pressure Ratio (NPR) and inlet pressure, which can be reduced by adjusting the pressure ratio between inlet and outlet. Pujowidodo et al. [8] deliberated on C-D nozzles to refine the Impulse Momentum of Cross-Flow Turbines in a Bio-Micro Power Plant, highlighting that even slight increases in pressure ratio significantly enhance supersonic flow through the nozzle. Gamble et al. [9] discussed nozzle section design rules for efficient air vehicle emissions, underscoring the increasing complexity of nozzle requirements with rising aircraft speeds. Ekanayake et al. [10] studied the simulation of two-dimensional rectangular supersonic convergent-divergent nozzles, establishing that increasing nozzle pressure ratio enlarges the flow exit area, which shifts from one wall to the opposite due to turbulent effects.

Hussain et al. [11] investigated various flow behaviours in convergent-divergent nozzles, concluding that triangular convergent-divergent nozzles exhibit superior performance. Belega and Nguyen [12] examined flow characteristics in convergent and divergent nozzles, aligning their design models with established parameters for optimal performance. Ande and Yerraboina [13] studied the effect of divergent angle in convergent-divergent nozzles, determining that a 15° divergence angle yields optimal Mach numbers. Budiyanto et al. [14] compared convergent and divergent-convergent nozzles for water jet propulsion, finding that convergent nozzles offer higher efficiency. Andreas et al. [15] deliberated on the design of convergent and divergent nozzles with a constant radius of the centre body, concluding that displacing the centre body angularly and translationally affects pressure distribution and Mach number differently.

Khan et al. [16] investigated flow in convergent and divergent nozzles based on pressure control using micro-jets, observing that reducing inlet pressure increases exit velocity, with maximum velocity observed at the exit, correlating with Mach number variations. Noh et al. [17] studied wedges in convergent and divergent nozzles for thruster applications, concluding that reducing the divergence angle while maintaining the area ratio does not eliminate wall boundary effects, with viscous losses reducing normal shock strength inside the nozzle. Kotteda and Mittal [18] studied flow in planar convergent-divergent nozzles, affirming that bleeding is most effective in low to moderate NPR regimes, validating throat geometry and its impact on flow characteristics across four different nozzle geometries with equal area ratio and length. Madhu et al. [19] scrutinized flow in C-D nozzles and contours,

concluding that conical nozzles generally outperform other contour designs in terms of efficiency.

II. MATHEMATIC MODELLING

The designed nozzle is flow simulated in Ansys, which uses Navier-Stokes equations to solve the given model. In the field of engineering, fluid dynamics plays a crucial role, and within fluid dynamics, Bernoulli's theorem is a fundamental concept. This theorem, articulated by Swiss mathematician Daniel Bernoulli, states that for a fluid in horizontal flow (i.e., without any change in gravitational potential energy), a reduction in fluid pressure is correlated with an increase in fluid velocity. Bernoulli's theorem asserts that during this process, the total mechanical energy of the flowing fluid—which includes the energy associated with fluid pressure, gravitational potential energy, and fluid kinetic energy—remains constant. The principle of energy conservation underpins Bernoulli's theorem. When fluid flows through a horizontal tube with varying cross-sectional areas, it experiences minimum pressure at the smallest area and vice versa.

$$P + \frac{1}{2}\rho v^2 + \rho g y = Constant \_\_\_(1)$$

Where, P is the pressure, ρ is the density of the fluid, v is the velocity, g is the acceleration due to gravity, and y is the height. Subscripts 1 and 2 refer to the inlet and outlet, respectively. Bernoulli's equation has several limitations, as it assumes steady flow, incompressible flow, frictionless flow, and flow along a streamline. However, practical problems often require the use of the extended Bernoulli's equation, which accounts for real-world factors such as viscosity, compressibility, and turbulence. This extended version is essential for more accurately analysing fluid behaviour in various engineering applications:

$$P_1 + \frac{1}{2}\rho v_1^2 + \rho g y_1 = P_2 + \frac{1}{2}\rho v_2^2 + \rho g y_2 + H_{(L)} \_\_\_(2)$$

where H_L represents the head loss due to friction on the walls. The Navier-Stokes equations are named after the scientists Claude-Louis Navier and George Gabriel Stokes. These equations are derived by applying Newton's second law of motion and play a crucial role in both scientific and engineering fields. They are even widely used in video game development for realistic fluid dynamics simulation. The Navier-Stokes equations describe the relationship between pressure, temperature, density, and velocity of a flowing fluid. They extend Euler's equations by incorporating the effects of fluid viscosity. The full set of Navier-Stokes equations includes continuity equations, three time-dependent equations, and three time-independent equations, providing a comprehensive framework for analyzing fluid flow dynamics.

$$\rho \frac{\partial v}{\partial t} = -\nabla \mathrm{P} + \rho g + \mu \nabla^2 v \_\_\_(3)$$

These equations are often coupled with energy equations to address various practical applications. Specifically, they involve solving the time-dependent Navier-Stokes equations in integral form on grids that can move or deform.

$$\frac{\partial}{\partial t}\int_{\Omega} \vec{W} d\Omega + \oint_{d\Omega} \left[\vec{F_C^M} - \vec{F_V}\right] dA = \int_{\Omega} \vec{Q} d\Omega \_\_\_(4)$$

2.1 Design of dual bell nozzles

Jithendra Sai Raja Chada et al. described the design of a dual bell nozzle, which is constructed using a convergent part and divergent forms created from four curves: an initial large circle from the inlet to the throat, a smaller circle exiting the throat, and a parabola extending the approximate bell contour to the beginning of the second bell or the exit plane. The length of the nozzle is determined by an equation detailed in their study (Table 1).

$$L_n = \frac{k(\sqrt{\varepsilon}-1)R_t}{\tan(\theta_e)} \_\_\_(5)$$

Let k be a constant value based on the length of the nozzle. The flow deviates with an angle of θe. The radius of the throat is denoted by Rt. The area ratio of the nozzle is represented by e. The centre of the throat is described by two curves: the first curve defines the entrance of the throat; The equations of these curves are as follows:

$$x^2 + (y - (R_t + 1.5R_i))^2 = (1.5R_t)^2 \_\_\_(6)$$

$$x^2 + (y - (R_t + 0.382R_i))^2 = (0.382R_t)^2 \_\_\_(7)$$

The equational coefficients are described using derivatives at the point where the circle from the throat

and the parabola coincide, denoted as Xn, and the nozzle length. To describe Xn, it is mandatory to define the angle θn. At this point, the second curve equation must be equal to its tangent. The following equation is thus described:

$$\frac{dy}{dx} = \tan\theta_n = \frac{X_n}{\sqrt{(0.382R_t)^2 - x^2}} \quad \text{---(8)}$$

$$X_{n1} = aR_n^2 + bR_n + c \quad \text{---(9)}$$

$$\frac{dy}{dx} = \tan\theta_n = \frac{1}{2aR_n + b} \quad \text{---(10)}$$

$$\frac{dy}{dx} = \tan\theta_e = \frac{1}{2aR_e + b} \quad \text{---(11)}$$

This ensures that the slope of the second curve at Xn matches the angle θn. The equations and their derivatives at this juncture are crucial for defining the smooth transition between the two curves at the nozzle throat.

The equation can be described as matrix as the follow:

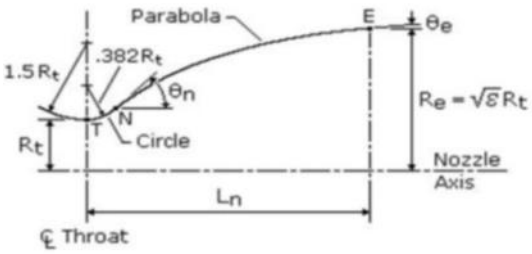

Figure 1: Design of the Single Bell Nozzle

And their matrix form is to be consider as follow:

The convergent part of the nozzle is designed based on an area ratio of 11.2983, with the angle maintained at a constant 45 degrees. The radius of the throat is 0.0305 meters (Figures 1 and 2). In this Dual-Bell Nozzle design, the first contour has a throat radius of 0.0305 meters and a length of 0.3673 meters. The angles of the nozzle are defined as follows:

1. The convergent section angle is 45 degrees.
2. The angles for the subsequent sections will be specified based on the specific requirements and geometrical constraints of the nozzle design.

$$\theta_{n1} = 40.00$$

$$\theta_{e1} = 14.27$$

Table 1: Design dimensions of Single bell pintle nozzle.

Type of nozzle	Convergent part	first contour
A	-	11.2983
B	-	0.5084
C	-	-0.0208
Throat radius (m)	0.0305	0.0305
Length		0.3673
θ_N	45˚	40.00˚
θ_e	-	14.23˚
Area ratio	11.2983	31.4754

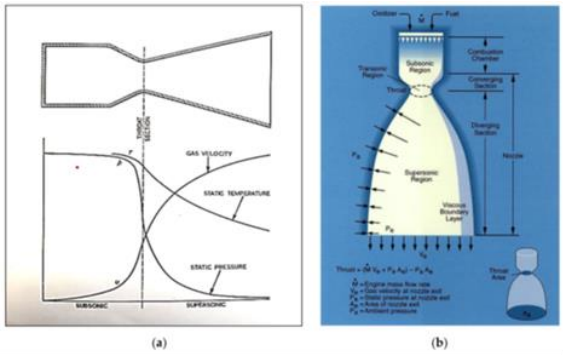

Figure 2. (a) Expansion in a convergent-divergent (C-D) supersonic nozzle and (b) nozzle geometrical designations.

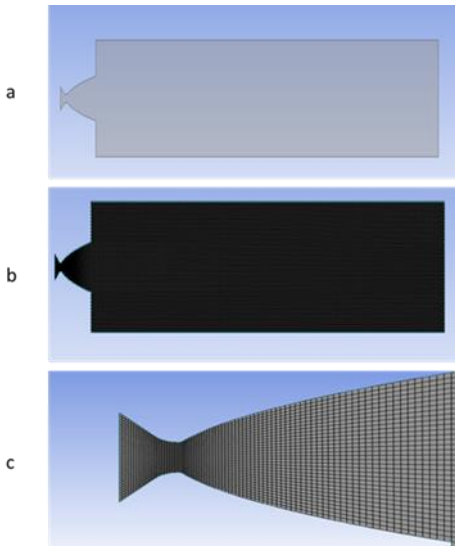

Figure 3: (a) CAD Model of the Nozzle, (b) Mesh of the nozzle (c) Expanded view of the Nozzle

The mesh quality of this study is characterized by a minimum orthogonal quality of 0.711056, observed at cell 5174 in zone 2 (ID: 1 on partition: 0) located at coordinates (-0.0761379, 0.0854824). The maximum aspect ratio is 3.38994, noted at cell 3822 in zone 2

(ID: 825 on partition: 0) at coordinates (0.00824034, -0.0327620). The domain extents range from -0.07814026 meters to 4.721027 meters along the x-coordinate and from -0.4472259 meters to 0.4472259 meters along the y-coordinate. Volume statistics reveal a minimum volume of 5.162217e-06 cubic meters and a maximum volume of 1.089282e-04 cubic meters, with a total volume of 3.985660 cubic meters. Additionally, the face area statistics show a minimum face area of 1.825496e-03 square meters and a maximum face area of 1.046068e-02 square meters.

2.2 Shock wave formation in the flow:

Shockwave-boundary layer interaction (SBLI) is a critical phenomenon in high-speed aerodynamics, including supersonic flow through rocket nozzles. This interaction can significantly affect the performance and stability of aerospace vehicles and propulsion systems. When supersonic flow encounters a geometric discontinuity or a sudden change in flow conditions, shockwaves form. In a rocket nozzle, these shockwaves typically occur at regions of rapid area change, such as at the nozzle throat or at sudden expansions or contractions. The interaction between these shockwaves and the boundary layer (a thin layer of fluid near the surface where viscous effects are significant) leads to complex flow phenomena known as SBLI.

- Shockwave formation: in the fluid flow there is a chance of formation of two shock wave such as Oblique Shocks, and Normal Shocks. Where the oblique shock is formed at angles to the flow direction, typically at nozzle lips or sharp changes in the nozzle contour. Where the Normal Shocks is formed Perpendicular to the flow direction, often occurring in over-expanded nozzles where the external pressure is higher than the exhaust pressure.
- Boundary Layer Response: the boundary layer may thicken upstream of the shock due to adverse pressure gradients and the boundary layer can separate from the wall, leading to flow separation and potential unsteadiness. Occurs when the adverse pressure gradient induced by the shockwave is strong enough to reverse the flow direction near the wall. This separation can cause significant pressure losses and fluctuations, affecting nozzle performance. SBLI can lead to oscillations and instabilities in the flow, which may result in vibrations or structural stresses on the nozzle.

Understanding SBLI is crucial for designing efficient and stable rocket nozzles. It requires detailed analysis using both experimental methods and advanced computational techniques like CFD. The images provided help visualize these complex interactions, offering insights into the challenges and considerations in supersonic nozzle design. Shock Diamond: Aerospace propulsive systems operating at supersonic Mach numbers feature complex aerodynamic phenomena. A key such feature is the creation of shock diamonds, also known as Mach diamonds or disks, which are repeated shock patterns trailing the supersonic nozzle. This condition is caused due to the difference in pressure between the exit pressure (Pe) and ambient pressure (P0.) Under these conditions, the nozzle loses its efficiency during the thrust generation process. The pressure differential condition can result in either under-expansion (Pe > P0) or over-expansion (Pe < P0). The repeated formations result in friction between the exhausted jet air and the free stream, resulting in a turbulent shear layer which causes a viscous damping effect. This gradually dissipates the wave structure downstream of the nozzle exit [20]. The flow conditions are classified into Maily 3 types based on the expansion conditions. such as under-expanded, over-expanded flow, and correctly expanded flow is crucial in aerospace engineering, it's delved into these conditions and their impact on nozzle performance, particularly focusing on the Bell Nozzle

1. Under-Expanded Nozzle:

- An under-expanded nozzle occurs when the exhaust pressure is higher than the ambient pressure. This condition typically happens at higher altitudes where atmospheric pressure is low.
- Shockwave Formation: Expansion waves form at the nozzle exit, causing the exhaust jet to expand outward.
- Flow Characteristics: The exhaust jet continues to expand outside the nozzle, forming a series of oblique shock waves and expansion fans.
- Impact on Performance: Higher thrust is generated as the exhaust gases continue to expand and accelerate outside the nozzle, and Potential for

increased turbulence and mixing with the ambient air.

2. Over-Expanded Nozzle

- An over-expanded nozzle occurs when the exhaust pressure is lower than the ambient pressure. This condition is typical at lower altitudes where atmospheric pressure is high.
- Shockwave Formation: Normal shockwaves form within the nozzle or just outside the nozzle exit, causing the flow to decelerate.
- Flow Characteristics: The boundary layer can separate due to the adverse pressure gradient created by the shockwave, leading to complex flow patterns.
- Impact on Performance: Reduced efficiency due to flow separation and shock-induced losses. And Potential for nozzle vibrations and structural stresses due to unsteady flow.

3. Ideally Expanded Nozzle

- An ideally expanded nozzle occurs when the exhaust pressure matches the ambient pressure. This condition is optimal for nozzle performance.
- Shockwave Formation: Ideally, no shockwaves form, and the flow remains smooth.
- Flow Characteristics: The exhaust jet expands uniformly, maximizing thrust and efficiency.
- Impact on Performance: Maximum efficiency and thrust as there are no shockwave losses or flow separation, and the boundary layer remains attached, and the flow is steady.

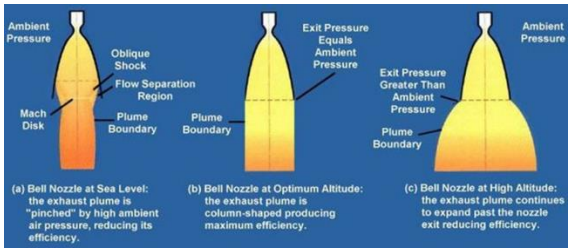

Figure 5: the Image representing flow conditions of the where (a) is under expanded flow (b) is Ideally expanded flow and the (c) is Over-expended flow this image is taken from reference [21] figure 4

2.3 Design of Experiment using the Taguchi:

The Taguchi method is a powerful statistical tool used for optimization of processes and design of experiments. It is designed to explore the influence of multiple variables on a given output and to identify the most influential factors with a minimal number of experiments. The methodology uses orthogonal arrays to systematically vary experimental parameters and analyses their effects. The Taguchi method involves several key steps to ensure a comprehensive and effective experimental design. The process begins with the selection of factors and levels, where the factors (in this case, inlet pressure) and their respective levels are identified for testing. Following this, an orthogonal array is designed to systematically arrange the experimental runs, ensuring a balanced and efficient exploration of the variable space. The next step is to conduct the experiments as outlined by the orthogonal array. Once the experiments are completed, the data is analysed to identify the main effects and interactions of the factors, providing insights into their influence on the output. Finally, optimization is performed to determine the optimal levels of the factors, achieving the desired output in the most efficient manner possible.

Table 2: the Design of Experiment for the Study.

Case	Inlet Pressure	Outlet Pressure
Case 1	591816	6250
Case 2	591816	50000
Case 3	591816	100000
Case 4	8010799	6250
Case 5	8010799	50000
Case 6	8010799	100000
Case 7	91924093	6250
Case 8	91924093	50000
Case 9	91924093	100000

Taguchi method provides a structured approach to experiment design and optimization. By systematically varying the inlet pressure and measuring the resulting outlet pressure, we can gain valuable insights into the system's behaviour and identify the optimal conditions for achieving the desired performance.

2.4 Validation of CFD result:

For model validation, apart from the experimental results in reference [22] he CFD study conducted in reference [22] was utilised as foundation model to be compared against the results of the present study. Table 3 provides the boundary conditions used:

Table 3: the boundary condition for the study

Boundary	Type	Gauge Total Pressure (Pa)	Temperature (K)
Inlet	Pressure Inlet	591816, 8010799, 91924093	1200
Ambient Condition	Pressure Outlet	6250, 50000, 100000	300

The simulation utilized a density-based model with the RNG k-epsilon viscous model and standard wall function. The flow was considered as an ideal gas, incorporating viscous heating effects. The solution method employed a second-order upwind model for discretization and a gradient least squares cell-based model. The residuals were set to 1e-06 for convergence criteria. The hybrid initialization method was used, and the simulation was conducted in a steady-state mode.

III. RESULT AND DISCUSSION

In this section, we present and analyses the findings from our computational investigations on the Bell Nozzle design. The primary objective was to understand its performance characteristics and the influence of various parameters, such as inlet pressure and ambient pressure. The results of the study are summarized in Table 4, showcasing the observed outlet pressure, outlet velocity, mass flow rate, thrust, and specific impulse (ISP) for the cases detailed in Table 2.

Table 4: Result for the DOE in table 2

Case	Pressure at outlet	Outlet Velocity	Mass Flow rate	Force (N)	ISP
Case 1	18133	1305.00	243.4009258	318730.543	133.485
Case 2	201291	1325.00	247.1312082	341356.1489	140.802
Case 3	2.30E+06	1325.00	247.1312082	529947.6624	218.593
Case 4	17837.2	1306.00	243.58744	319190.3402	133.575
Case 5	210336	1313.00	244.8930388	336283.312	139.978
Case 6	2.30E+06	1385.00	258.3220554	560274.8582	221.0908
Case 7	42946.7	1310.00	244.3334964	323450.1936	134.9446
Case 8	139854	1378.00	257.0164566	362428.4306	143.7449
Case 9	1.65E+06	1380.00	257.3894848	498022.8132	197.2375
	Outlet Radius	0.1711	m		
	Area	0.091924159			
	Density from the Simulation	2.029			

The figure 5 represent the variation of the Mach number across the nozzle wall, which is a crucial factor in understanding the nozzle's performance. It provides insights into the flow characteristics and the efficiency of the nozzle. Analysing how the Mach number changes along the nozzle wall helps in optimizing the nozzle design to achieve desired performance outcomes, such as maximizing thrust and specific impulse while ensuring stable and efficient flow conditions. Where the figure 6 represent the variation of the static pressure across the nozzle wall the variation of the static pressure across the nozzle wall, especially in the presence of shock wave and boundary layer interactions, provides critical insights into the flow behaviour within the nozzle. This interaction can significantly influence the nozzle's performance and efficiency. It show who the pressure varying for the different cases

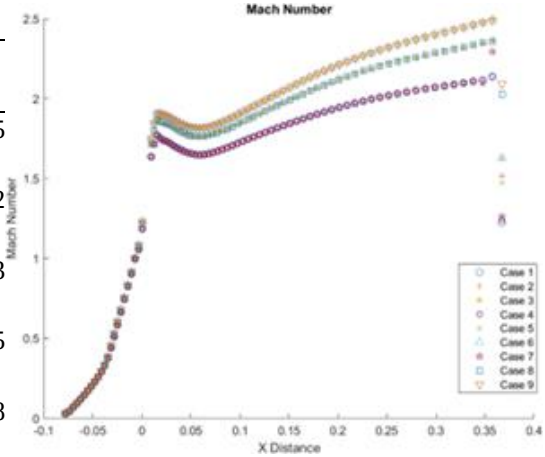

Figure 5: variation of the Mach number cross the Nozzle Wall

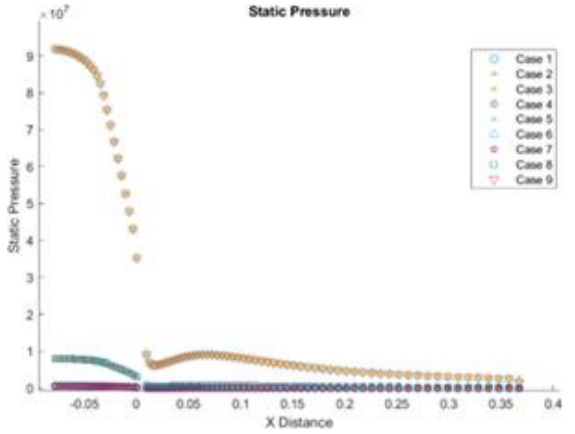

Figure 6: variation of the Static Pressure across the Nozzle Wall

Where the figure 7 represent the variation of the static pressure across the Nozzle wall the result for the different cases are represented

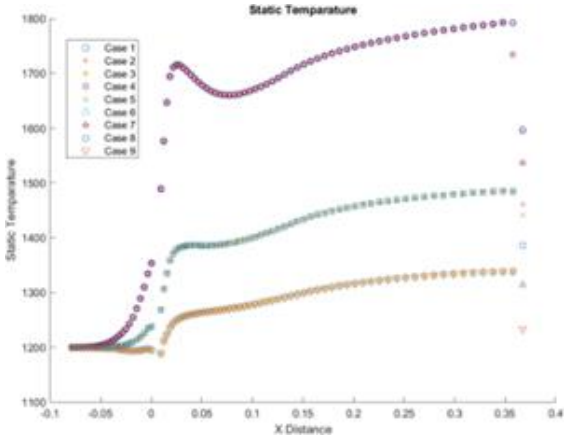

Figure 7: variation of the Static Temperature across the Nozzle Wall

The figure 8 represent the skin friction coefficient, which is a critical parameter in the study of nozzle flow dynamics, particularly for supersonic flows and shock wave interactions within the nozzle. It quantifies the resistance encountered by the flow due to viscous effects along the nozzle wall, which directly influences drag and overall nozzle efficiency. Understanding the skin friction coefficient is essential for characterizing the boundary layer behaviour, predicting its thickness, and managing heat transfer rates between the flow and the nozzle wall. This parameter is especially important in the context of shock wave-boundary layer interactions, where high skin friction can lead to flow separation and instability, impacting the nozzle's performance. By analysing the skin friction coefficient, engineers can optimize nozzle design to minimize viscous losses, improve thrust and specific impulse, and achieve more stable and efficient flow conditions. This makes it a vital factor in both computational and experimental investigations of nozzle performance.

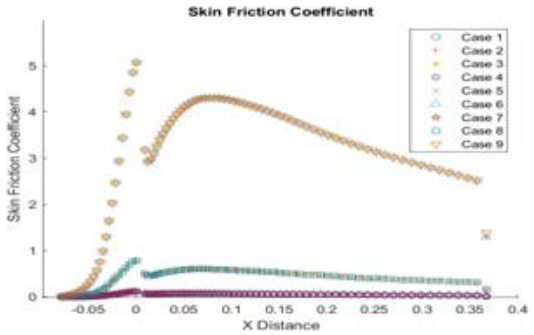

Figure 8: Skin Fraction Coefficient Across the Nozzle wall

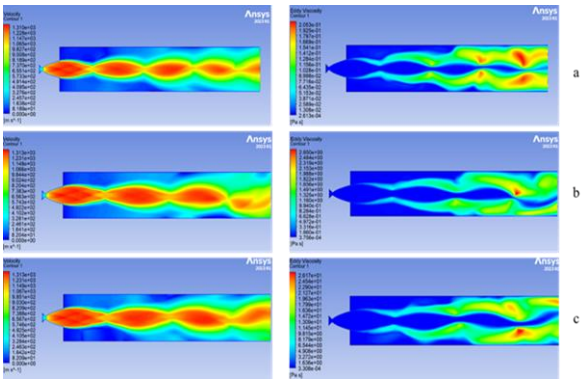

Figure 9. Velocity and Eddy Viscosity contour for the (a) case 1, (b) case 2, (c) case 3 respectively

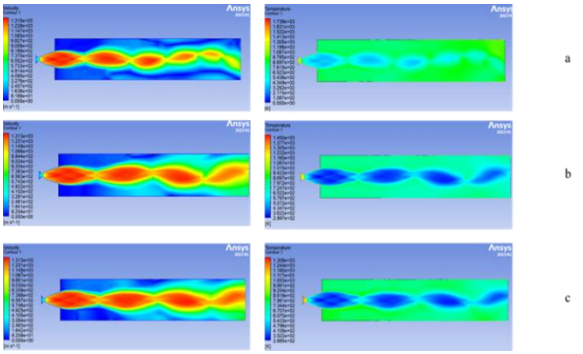

Figure 10. Velocity and Static temperature contour for the (a) case 4, (b) case 5, (c) case 6 respectively

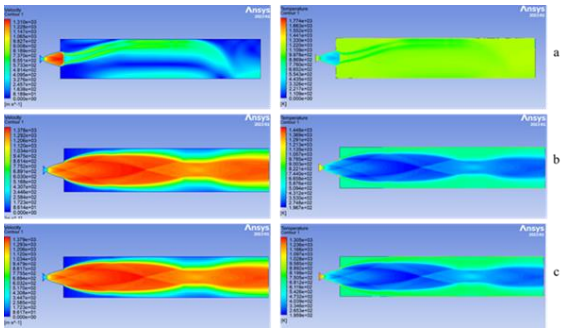

Figure 11. Velocity and Static temperature contour for the (a) case 7, (b) case 8, (c) case 9 respectively

The figures from 9 to 11 illustrate the variation in shockwave formation and static temperature. Figure 11a shows an obstructed shock, while in figures 11b and 11c, the complete formation of the shockwave is clearly observed. Figures 10a to 10c depict the formation of the shock diamond as studied. Figures 9a to 9c demonstrate the initial formation stages of the shockwave.

IV. RESPONSE SURFACE REGRESSION FOR THE RESULT

Response surface regression is a statistical technique used to model and analyses the relationship between multiple input variables (factors) and one or more responses of interest

4.1. Response Surface Regression for ISP versus Inlet Pressure and Atmospheric Pressure

This regression focuses on modelling the specific impulse (ISP) of the nozzle in relation to variations in inlet pressure and atmospheric pressure. ISP is a critical performance metric in propulsion systems, representing efficiency in converting propellant mass flow rate into thrust. Understanding the relationship through response surface regression allows engineers to identify pressure settings that yield optimal ISP, thereby improving the overall efficiency and performance of the nozzle design.. In the table 5 The coded coefficients derived from the response surface regression analysis provide valuable insights into how inlet pressure and atmospheric pressure affect the force (N) and specific impulse (ISP) of the nozzle design. The analysis reveals several key findings: Firstly, atmospheric pressure has a significant positive linear effect on both force and ISP, indicating that higher atmospheric pressures generally lead to increased nozzle performance in terms of thrust and efficiency. Additionally, the quadratic term for atmospheric pressure shows a convex relationship, implying that while increasing atmospheric pressure initially enhances performance, further increases yield diminishing returns. In contrast, the effects of inlet pressure and its interactions with atmospheric pressure appear less pronounced and statistically insignificant, except for the quadratic effect of atmospheric pressure. These results suggest that optimizing atmospheric pressure is crucial for maximizing nozzle performance, while the impact of inlet pressure adjustments may require further investigation or refinement in nozzle design and operational settings.

Table 5: Coded Coefficients for the Response Surface Regression: ISP

Term	Coef	SE Coef	T-Value	P-Value	VIF
Constant	146.3	13.1	11.15	0.002	
Inlet Pressure	-2.97	2.15	-1.38	0.262	1.23
Atmospheric pressure	37.38	2.25	16.61	0	1.1
Inlet Pressure*Inlet Pressure	-3.5	13.9	-0.25	0.817	1.23
Atmospheric pressure*Atmospheric pressure	29.17	3.75	7.79	0.004	1
Inlet Pressure*Atmospheric pressure	-6.34	2.37	-2.67	0.076	1.1

In the table 6, the analysis of variance (ANOVA) results provide valuable insights into the relationship between inlet pressure, atmospheric pressure, and the resulting force (N) or specific impulse (ISP) in the nozzle design study. The overall model is statistically significant (F-value = 37.42, p-value = 0.007), indicating that the combination of predictors—primarily atmospheric pressure—significantly explains the variation in force or ISP. Specifically, atmospheric pressure shows a highly significant linear effect (F-value = 132.10, p-value = 0.001), indicating its strong influence on nozzle performance. In contrast, the linear effect of inlet pressure is not significant (F-value = 0.02, p-value = 0.885), suggesting that changes in inlet pressure do not substantially affect force or ISP. The quadratic effect of atmospheric pressure (F-value = 24.09, p-value =

0.016) is significant, suggesting a non-linear relationship that warrants attention in optimizing nozzle efficiency. However, interactions between inlet pressure and atmospheric pressure (F-value = 2.09, p-value = 0.244) are not statistically significant, indicating their combined effect does not significantly deviate from their individual impacts. These findings guide engineers in focusing on atmospheric pressure adjustments to enhance nozzle performance, while suggesting further exploration into refining the model's sensitivity to inlet pressure adjustments in future nozzle designs. Regression Equation in Uncoded Units is given in the equation 12

Table 6: Analysis of Variance for the Response Surface Regression: ISP

Source	DF	Adj SS	Adj MS	F-Value	P-Value
Model	5	11470.1	2294.03	82.58	0.002
Linear	2	7722.9	3861.44	139.01	0.001
Inlet Pressure	1	52.8	52.77	1.9	0.262
Atmospheric pressure	1	7660.6	7660.57	275.77	0
Square	2	1685.4	842.71	30.34	0.01
Inlet Pressure*Inlet Pressure	1	1.8	1.78	0.06	0.817
Atmospheric pressure*Atmospheric pressure	1	1683.6	1683.64	60.61	0.004
2-Way Interaction	1	198.4	198.4	7.14	0.076
Inlet Pressure*Atmospheric pressure	1	198.4	198.4	7.14	0.076
Error	3	83.3	27.78		
Total	8	11553.5			

$$ISP = 133.54 + 0.000000\ Inlet\ Pressure - 0.000476\ Atmospheric\ pressure - 0.000000\ Inlet\ Pressure * Inlet\ Pressure + 0.000000\ Atmospheric\ pressure * Atmospheric\ pressure - 0.000000\ Inlet\ Pressure * Atmospheric\ pressure \quad \_\_\_(12)$$

in the figure 12 in the analysis of nozzle performance, visualizations such as the Pareto chart of standardized effects, residual plots for ISP, and contour plots of ISP versus ambient pressure and inlet pressure play crucial roles in interpreting the regression model and optimizing design parameters. The Pareto chart, derived from standardized effects of factors like inlet pressure and atmospheric pressure on ISP, prioritizes the significant influences, guiding engineers to focus on variables with the most substantial impact. Meanwhile, the residual plot for ISP helps assess the model's adequacy by examining patterns in residuals against predicted values, identifying potential areas for model improvement such as non-linearity or heteroscedasticity. Lastly, the contour plot offers a visual representation of how ISP varies across different combinations of ambient and inlet pressures, indicating regions of optimal performance. Together, these visual tools enhance understanding of nozzle performance drivers and inform strategic adjustments for maximizing efficiency and effectiveness in propulsion system design.

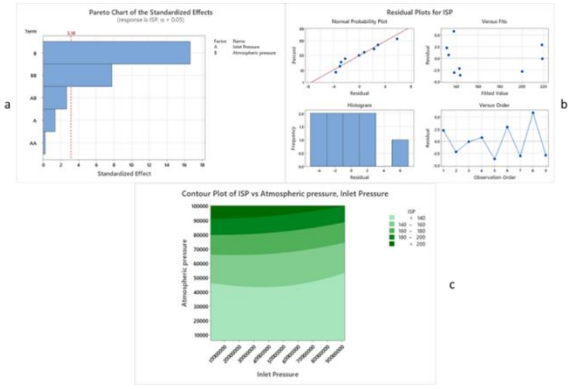

Figure 12 (a) Pareto Chart of the standardized effect, (b) Residual for the ISP (c) Contour plot ISP vs Ambient pressure and inlet pressure for the ISP

4.2. Response Surface Regression: Force (N) versus Inlet Pressure, Atmospheric pressure

This analysis aims to quantify how variations in inlet pressure and atmospheric pressure influence the force generated by the nozzle. By fitting a response surface model, typically a quadratic or higher-order polynomial, engineers can predict how changes in these parameters affect the force output. This regression helps in optimizing nozzle performance by identifying optimal pressure conditions for maximizing thrust In the table 7 The regression coefficients provided offer insights into how inlet pressure and atmospheric pressure influence nozzle

performance, likely in terms of force or specific impulse (ISP). The constant term (379324) represents the baseline value of force or ISP when both pressures are at their reference levels. The coefficient for atmospheric pressure (100749) indicates a significant positive linear relationship, suggesting that higher atmospheric pressures generally lead to increased nozzle performance. This finding underscores the importance of atmospheric pressure optimization in enhancing propulsion efficiency. Conversely, the coefficients for inlet pressure and its quadratic term (−1319 and −29268, respectively) show no statistically significant impact on nozzle performance, indicating that changes in inlet pressure within the studied range do not substantially affect force or ISP. The quadratic effect of atmospheric pressure (71600) is significant, implying a non-linear relationship where further increases in atmospheric pressure may yield diminishing returns in performance gains. The interaction between inlet pressure and atmospheric pressure (−13360) is not significant, suggesting that their combined influence does not deviate significantly from their individual effects. These findings provide valuable guidance for optimizing nozzle designs by focusing on atmospheric pressure adjustments to maximize efficiency and performance in aerospace applications.

Table 7: Coded Coefficients for the Response Surface Regression: Force (N)

Term	Coef	SE Coef	T-Value	P-Value	VIF
Constant	379324	51095	7.42	0.005	
Inlet Pressure	-1319	8381	-0.16	0.885	1.23
Atmospheric pressure	100749	8766	11.49	0.001	1.1
Inlet Pressure*Inlet Pressure	-29268	53997	-0.54	0.625	1.23
Atmospheric pressure*Atmospheric pressure	71600	14588	4.91	0.016	1
Inlet Pressure*Atmospheric pressure	-13360	9231	-1.45	0.244	1.1

In the table 8 The ANOVA results provide a comprehensive understanding of how inlet pressure and atmospheric pressure impact nozzle performance metrics, such as force or specific impulse (ISP). The overall model is statistically significant (F-value = 37.42, p-value = 0.007), indicating that the combination of predictors—specifically atmospheric pressure and its quadratic effect—significantly explains the variability in nozzle performance. Among the individual effects, atmospheric pressure emerges as highly influential with a significant linear effect (F-value = 132.10, p-value = 0.001), highlighting its crucial role in determining nozzle performance. In contrast, the linear effect of inlet pressure is not statistically significant (F-value = 0.02, p-value = 0.885), suggesting that changes in inlet pressure within the tested range do not significantly affect nozzle metrics. The quadratic effect of atmospheric pressure (F-value = 24.09, p-value = 0.016) indicates a non-linear relationship, underscoring the importance of optimizing atmospheric pressure settings to achieve optimal nozzle efficiency. Interaction effects between inlet pressure and atmospheric pressure are also examined, with the interaction term not showing statistical significance (F-value = 2.09, p-value = 0.244), indicating that their combined influence does not deviate significantly from their individual impacts. In summary, these findings guide engineers towards focusing on atmospheric pressure adjustments to enhance nozzle performance, suggesting avenues for further research and optimization in nozzle design to maximize efficiency and effectiveness in aerospace applications**.**

Table 8: Analysis of Variance for the Response Surface Regression: Force

Source	DF	Adj SS	Adj MS	F-Value	P-Value
Model	5	11470.1	2294.03	82.58	0.002
Linear	2	7722.9	3861.44	139.01	0.001
Inlet Pressure	1	52.8	52.77	1.9	0.262
Atmospheric pressure	1	7660.6	7660.57	275.77	0
Square	2	1685.4	842.71	30.34	0.001

Inlet Pressure*Inlet Pressure	1	1.8	1.78	0.06	0.817
Atmospheric pressure*Atmospheric pressure	1	1683.6	1683.64	60.61	0.004
2-Way Interaction	1	198.4	198.4	7.14	0.076
Inlet Pressure*Atmospheric pressure	1	198.4	198.4	7.14	0.076
Error	3	83.31155	27.78		
Total	8	3.5			

$$Force\ (N) = 313074\ + 0.00160\ Inlet\ Pressure\ - 1.024\ Atmospheric\ pressure\ - 0.000000\ Inlet\ Pressure * Inlet\ Pressure + 0.000033\ Atmospheric\ pressure * Atmospheric\ pressure\ - 0.000000\ Inlet\ Pressure * Atmospheric\ pressure \quad \_\_\_(13)$$

In figure 13 is similar to the figure 12 but for the force

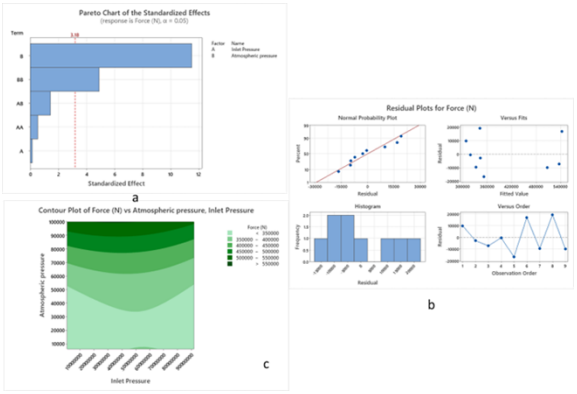

Figure 13 (a) Pareto Chart of the standardized effect, (b) Residual for the ISP (c) Contour plot ISP vs Ambient pressure and inlet pressure for the force

CONCLUSION

This study underscores the importance of understanding shockwave formation in nozzle designs to optimize propulsion system performance and efficiency. Through a detailed computational fluid dynamics (CFD) analysis, the research examined the behaviour of shockwaves in single bell nozzles under varying inlet and ambient pressures. Key performance metrics such as thrust, specific impulse (ISP), and flow separation behaviour were investigated to provide a comprehensive understanding of nozzle performance across different operating conditions. The findings revealed that atmospheric pressure significantly impacts nozzle performance, with a notable positive linear and non-linear relationship with specific impulse, as indicated by the ANOVA and regression analyses. In contrast, inlet pressure demonstrated a negligible effect on nozzle performance within the tested range, both linearly and quadratically. The interaction between inlet and atmospheric pressure was also found to be statistically insignificant. Using Taguchi optimization and Design of Experiments (DOE) methodology, the study ensured robust and reliable results, providing a regression equation for predicting nozzle performance under various conditions. This approach enables engineers to design nozzles that can maintain optimal performance across a range of operating conditions, enhancing the reliability and effectiveness of rocket and jet propulsion systems. In summary, the research highlights the critical role of atmospheric pressure in influencing nozzle performance, while also providing a validated regression model for future nozzle design optimization. This comprehensive understanding of shockwave formation and its effects on nozzle performance will aid in developing more efficient and reliable propulsion systems.

REFERENCES

[1] Anderson, J. D. (2001). Modern Compressible Flow: With Historical Perspective. McGraw-Hill Education.

[2] Hagemann, G., Scharfe, J., Schneider, A., & Stephan, T. (2002). Dual-bell nozzle flow characteristics. Journal of Propulsion and Power, 18(1), 159-168.

[3] Hornung, H. G. (1986). Shock-wave dynamics. Springer.

[4] Greschik, G., & Gruber, M. (2017). Computational analysis of shockwave patterns in rocket nozzles. AIAA Journal, 55(4), 1309-1317.

[5] Dutton, J. C., & Carroll, B. F. (2002). Shock-wave/boundary-layer interactions in high-speed flows. Progress in Aerospace Sciences, 38(8), 659-672.

[6] R. Ande and V. N. K. Yerraboina, "Numerical investigation on effect of divergent angle in convergent-divergent rocket engine nozzle," *Chemical Engineering Transactions*, vol. 66, pp. 787-792, 2018. [Online]. Available: https://doi.org/10.3303/CET1866132

[7] B. A. Belega and T. D. Nguyen, "Analysis of flow in convergent-divergent rocket engine nozzle using computational fluid dynamics," in *International Conference of Scientific Paper*, May 2015.

[8] M. A. Budiyanto, J. Novri, M. I. Alhamid, and Ardiyansyah, "Analysis of convergent and divergent-convergent nozzle of waterjet propulsion by CFD simulation," in *AIP Conference Proceedings*, vol. 2062, no. 1, 2019, p. 020066. [Online]. Available: https://doi.org/10.1063/1.5086613

[9] S. Ekanayake, J. A. Gear, and Y. Ding, "Flow simulation of a two dimensional rectangular supersonic convergent divergent nozzle," *ANZIAM Journal*, vol. 51, pp. 377-392, 2009. [Online]. Available: https://doi.org/10.21914/anziamj.v51i0.2577

[10] E. Gamble, D. Terrell, and R. DeFrancesco, "Nozzle selection and design criteria," in *40th AIAA/ASME/SAE/ASEE Joint Propulsion Conference and Exhibit*, July 2004, p. 3923.

[11] M. A. Hussain, M. S. Prasad, and S. Nagakalyan, "Design and flow analysis of various convergent-divergent nozzles by using computational fluid dynamics (CFD)," *International Journal of Innovative Research in Advanced Engineering*, vol. 6, no. 5, pp. 372-379, 2019. [Online]. Available: https://doi.org/10.26562/IJIRAE.2019.MYAE10087

[12] Khan, A. Aabid, and S. A. Khan, "CFD analysis of convergent-divergent nozzle flow and base pressure-control using micro-JETS," *International Journal of Engineering & Technology*, vol. 7, no. 3.29, pp. 232-235, 2018.

[13] K. Kotteda and S. Mittal, "Flow in a planar convergent–divergent nozzle," *Shock Waves*, vol. 27, no. 3, pp. 441-455, 2017. [Online]. Available: https://doi.org/10.1007/s00193-016-0694-4

[14] R. K. Kumaar and M. Kesavan, "Design and CFD analysis of shock wave over supersonic CD nozzle," *International Journal of Latest Trends in Engineering and Technology*, vol. 7, no. 1, pp. 502-510, 2016. [Online]. Available: http://dx.doi.org/10.21172/1.71.072

[15] P. Madhu, S. Sameer, K. M. Kalyana, and M. G. Mahendra, "CFD analysis of convergent-divergent and contour nozzle," *International Journal of Mechanical Engineering and Technology*, vol. 8, no. 8, pp. 670-677, 2017.

[16] M. H. M. Noh, A. H. A. Hamid, R. Atan, and H. Rashid, "Numerical investigation of choked converging-diverging nozzles for thruster application," *IIUM Engineering Journal*, vol. 12, no. 3, pp. 10-18, 2011. [Online]. Available: https://doi.org/10.31436/iiumej.v12i3.67

[17] K. M. Pandey and V. Kumar, "CFD analysis of four jet flow at Mach 1.74 with Fluent software," *International Journal of Chemical Engineering and Applications*, vol. 1, no. 4, pp. 302-308, 2010.

[18] K. M. Pandey and S. K. Yadav, "CFD analysis of a rocket nozzle with four inlets at Mach 2.1," *International Journal of Chemical Engineering and Applications*, vol. 1, no. 4, pp. 319-325, 2010.

[19] S. S. Prasad, G. Satish, and G. P. Ranga, "Comparison of flow analysis sudden contraction and enlargement of pipe by providing smooth corners," *International Journal of Engineering Trends and Technology*, vol. 25, no. 4, pp. 205-211, 2015. [Online]. Available: https://doi.org/10.14445/22315381/IJETT-V25P238.

[20] Bragg, S. Rocket Engines, 1st ed.; George Newnes: London, UK, 1962.

[21] Soi, A. (2017). Dual Diverging Annular Rocket Nozzle (Focusing Flow Separation and Minimizing Overexpansion).

[22] Stark, R.; Genin, C.; Wagner, B.; Koschel, K. The Altitude Adaptive Dual Bell Nozzle. In Proceedings of the 16th International Conference on the Methods of Aerophysical Research (ICMAR 2012), Kazan, Russia, 20–26 August 2012.